Journal of Environmental Economics & Chemical Processes (JEECP)

https://doi.org/10.22034/jeecp.2025.735058

Journal homepage: *WWW.JEECPJournal.com*

Journal of Environmental Economics & Chemical Processes (JEECP)

ORIGINAL RESEARCH PAPER

Comparative Study of Isobutyl Acetate and Ethyl Acetate as Azeotrope-Breaking Agents in Acetic Acid–Water Separation

Mahyar Daneshyar[a], Sara Abbasi[b], Mohammad Reza Khosravi-Nikou[b,*]

[a] *Shahid Tondgouyan Petrochemical Company, Mahshahr, Iran.*
[b] *Department of Gas Engineering, Ahvaz Faculty of Petroleum, Petroleum University of Technology, Ahvaz, Iran.*

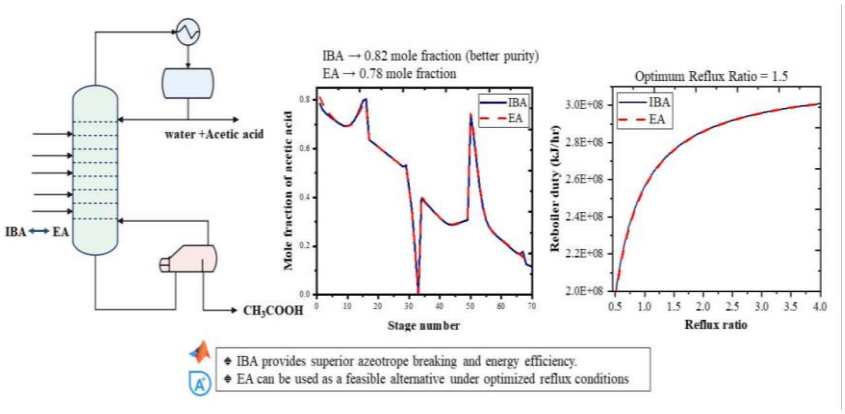
P A P E R I N F O

Paper history:
Received 11/16/2025
Accepted in revised form 01/20/2026

***Keywords*:**
Acetic Acid
Water Separation
Distillation Column
Aspen Plus
MATLAB
Isobutyl Acetate
Ethyl Acetate
Azeotropic Separation

A B S T R A C T

Acetic acid is one of the most important industrial chemicals due to its broad applications and high economic value. However, its separation from water remains a major challenge because of azeotrope formation, which restricts the performance of conventional distillation methods. In this study, the separation of acetic acid and water in a distillation column was simulated and analyzed to evaluate and optimize the performance of an industrial-scale process. The process modeling was carried out using Aspen Plus (Version 12) employing a RadFrac distillation column with 72 theoretical stages and a kettle-type reboiler, while MATLAB was utilized for post-simulation data analysis and process optimization. The effects of two different entrainers-isobutyl acetate (IBA) and ethyl acetate (EA)-on separation efficiency and energy consumption were investigated in detail. Simulation results indicated that using IBA achieved a bottom product purity of 0.82 mole fraction, closely matching the design target of 0.85, whereas substituting it with EA slightly decreased the purity to 0.78, corresponding to a 4% reduction in separation efficiency. Temperature and composition profiles confirmed that IBA provided more stable operation and better agreement with expected industrial performance. Furthermore, MATLAB-based optimization revealed that a reflux ratio of 1.5 offers the most favorable trade-off between acetic acid purity and reboiler energy duty, minimizing energy consumption without sacrificing separation quality. The findings demonstrate that isobutyl acetate remains the superior entrainer for acetic acid–water separation, while ethyl acetate can serve as a viable alternative under optimized operating conditions without requiring equipment modification.



1. Introduction

Acetic acid is one of the most important industrial chemicals, widely employed in the production of vinyl acetate, acetate esters, cellulose acetate, and various solvents. High-purity acetic acid is essential in these applications, as impurities can affect the physical and chemical properties of the final product and reduce its performance. Contaminants such as water, acetaldehyde, formic acid, and volatile organic compounds may alter the boiling point, viscosity, and acidity of acetic acid. In many chemical processes and reactions, water-free acetic acid is required because the hydroxyl groups in water can interfere with acetic acid, lowering reaction efficiency and generating unwanted by-products. Pure molten acetic acid is also used as a solvent in the production of terephthalic acid, the primary raw material for polyethylene terephthalate (PET) [1].

There are three main techniques typically applied for the separation of acetic acid and water: conventional distillation, azeotropic distillation, and extractive distillation [2-4]. Conventional distillation is straightforward and easy to operate, but it requires a large number of trays and involves high energy

* Corresponding author: Mohammad Reza Khosravi-Nikou
E-mail address: mr.khosravi@put.ac.ir
ISSN: 3116-0050
URL: https://www.jeecpjournal.com/article_735058.html

Please cite this article as: M. Daneshyara, S. Abbasib, M. R. Khosravi-Nikoub, *Journal of Environmental Economics & Chemical Processes (JEECP)*, 2026, 3(1), 1-9.

/© 2026 The Author(s). Published by Institute of Power, Movement, and Innovative Insight

consumption. Azeotropic distillation reduces the number of trays compared to conventional distillation; however, it requires a significant amount of entrainer, which must be vaporized in the column, increasing energy usage. Extractive distillation, on the other hand, avoids vaporizing the separating agents, leading to lower energy requirements. Nevertheless, in many industrial applications, azeotropic distillation with a suitable entrainer remains the preferred method, as it effectively breaks the acetic acid–water azeotrope and allows for high-purity acetic acid recovery.

Acetic acid and water form a low-boiling azeotrope, which prevents the attainment of high-purity acetic acid by conventional distillation. This challenge arises from the small difference in composition between the liquid and vapor phases near the water-rich region, often referred to as the "pinch point", making the separation process more difficult. Therefore, it is more common to use a third component, known as an entrainer, along with a heterogeneous azeotropic distillation system to achieve effective separation. In many studies, the use of an entrainer in the design of acetic acid dehydration systems has been extensively investigated. Before 1932, ethylene dichloride was commonly used as the entrainer; later, n-propyl acetate and n-butyl acetate were adopted to reduce the reflux of organic components and to decrease the reboiler heat load in the dehydration column [5]. In a study, ethyl acetate was employed as an entrainer in a complete process design for acetic acid dehydration using a heterogeneous azeotropic distillation system with integrated heat recovery [6]. Additionally, geometric design methods have been proposed for optimizing the dehydration column when using n-butyl acetate as the entrainer [7]. Other investigations also recommend n-butyl acetate as a suitable entrainer for acetic acid dehydration [8]. In a study [9] the effects of three different entrainers were examined through modeling and concluded that the optimal condition occurs when the bottom product is pure acetic acid and losses of this valuable compound in the overhead product are minimized. Outtmer [5] described a heterogeneous azeotropic distillation system that includes a dehydration column, a decanter, and a water column for separating water and acetic acid. In earlier studies, ethylene dichloride was used as the entrainer, while later, n-propyl acetate and n-butyl acetate were employed to reduce organic reflux and reboiler heat load in the dehydration column. In another study, ethyl acetate was used as an entrainer in a complete design of an acetic acid dehydration process using heterogeneous azeotropic distillation with heat integration [10]. To address the challenges of separating azeotropic mixtures, various strategies have been proposed, including forming an azeotrope with an entrainer, using additive compounds, and reactive or extractive distillation. The choice of method depends on the separation approach and economic parameters [11]. In a further report, the most appropriate entrainer, (p-xylene) for the acetic acid dehydration system was selected from among acetate candidates [9].

In this study, the parameter values for two entrainers-isobutyl acetate and ethyl acetate-were determined and compared to evaluate their effectiveness in acetic acid-water separation. A heterogeneous azeotropic distillation column was designed to achieve a high-purity acetic acid product at the bottom, while the overhead stream consisted mainly of the water-entrainer azeotrope, which corresponds to the lowest-boiling mixture in the system. Therefore, the main design objective was to maximize acetic acid purity in the bottom product. Thermodynamic and equilibrium data, including azeotropic compositions [12], vapor-liquid equilibrium (VLE) [13], binary and ternary liquid-liquid equilibrium (LLE) [14], activity coefficient models for ternary liquid-liquid-vapor systems [15], and the second virial coefficient with temperature-dependent parameters [11] were adopted from literature sources. A key strength of this work lies in the integration of mass and energy balance equations with thermodynamic models, implemented numerically in MATLAB, which distinguishes it from conventional simulation-based studies. The developed numerical framework allows simultaneous solution of total and component mass balances along with the overall energy balance for the column, followed by parameter optimization to enhance the acetic acid-water separation efficiency and reduce energy consumption. In addition, the distillation process was simulated using Aspen Plus (Version 12) with a RadFrac equilibrium model consisting of 72 theoretical stages, a kettle-type reboiler, and a total condenser under steady-state conditions. The NRTL activity coefficient model was applied to represent the non-ideal phase behavior of the acetic acid-water-entrainer system. This simulation framework enabled prediction of temperature, composition, and flow rate profiles throughout the column, providing reliable validation of the MATLAB-based numerical modeling results and ensuring consistency with expected industrial-scale performance. Overall, this study combines numerical modeling and process simulation to identify optimal operating parameters and evaluate the feasibility of replacing isobutyl acetate with ethyl acetate as an entrainer in acetic acid-water azeotropic distillation.

2. Methodology

2.1. Mathematical Modeling Using MATLAB

In order to perform numerical modeling of the azeotropic distillation of the water-acetic acid system, a comprehensive understanding of the governing principles, thermodynamic relations, and balance equations is required. The separation of water and acetic acid in such systems involves complex phase equilibria, particularly due to the azeotropic behavior, and thus careful formulation of the mathematical model is essential. For accurate simulation, mass and energy balances must be applied to each section of the distillation column, while the corresponding equilibrium relations are incorporated into the model. The overall performance of the column is then obtained by combining the local balances from different stages. This approach ensures that the model can correctly predict the behavior of the column under various operating conditions. The system under investigation is the distillation column, where a feed mixture of water and acetic acid enters the column and purified acetic acid is obtained from the bottom of the column, while the overhead stream, containing a mixture of water and acetic acid, is directed to another distillation column for further purification of water. Additionally, part of the overhead product is recycled as reflux to maintain separation efficiency. The main strategy adopted for breaking the azeotropic constraint in this process is the addition of an entrainer. Accordingly, the feed to the column consists of the liquid water-acetic acid mixture along with the selected entrainer. In this study, the influence of isobutyl acetate and ethyl acetate as entrainers is investigated. These compounds interact preferentially with water molecules, thereby releasing the acetic acid molecules from the azeotropic constraint. As a result, acetic acid can be more effectively separated and withdrawn from the bottom of the column at high purity. The following subsections present the detailed mathematical formulation of the mass and energy balances, vapor-liquid equilibrium relations, and the final numerical implementation using MATLAB.

The steady-state modeling of a distillation column is primarily derived from overall mass and energy balances, which requires a proper understanding of the column configuration to establish the governing mathematical equations. The model is formulated using the so-called MESH equations, which consist of material balances, phase equilibrium relations, mole fraction summation constraints, and heat (energy) balances. To keep the formulation as general as possible, the model assumes that feed streams may enter at any stage, while the outlet streams (distillate and bottoms) may leave in liquid, vapor, or a combination of both phases [16]. Figure 1 illustrates the overall distillation column layout, whereas Figure 2 depicts the input and output streams for an individual stage.

In this formulation, F_j epresents the feed flow rate entering stage j, while Q_j denotes the heat duty associated with that stage (with the convention that heat is considered to leave the stage). The liquid flow rate exiting stage j and entering stage $j+1$ is expressed as L_j, and the vapor flow rate leaving stage j and entering stage $j-1$ is given by V_j Additionally, U_j and W_j correspond to the liquid and vapor side streams, respectively, that exit stage j. These side draws can be used to describe the distillate and bottoms streams-denoted as D and B-which may consist of liquid (L_D, L_B) and/or vapor (V_D, V_B) phases, such that $D=L_D+V_D$ and $B=L_B+V_B$. The column is assumed to have n stages, numbered sequentially from the condenser ($j=1$) down to the reboiler ($j=n$). The side streams may be withdrawn from any stage, including the top or bottom of the column. However, some care must be taken when using this diagram (Figure 2) as the basis for mass and energy balance derivations. Specifically, since there is no stage 0, the streams U_0 and L_0 leaving that stage, as well as the stream V_1 entering it, do not exist. Similarly, because there is no stage $n+1$, the streams V_{n+1} and W_{n+1} leaving that stage, and the stream L_n entering it, are also nonexistent. Therefore, the following boundary conditions must be imposed: $W_{n+1} = V_{n+1} = L_n = U_0 = L_0 = V_1 = 0 \cdot$

Thus, the mass balance for any given stage j can be expressed as follows.

$$F_j + V_{j+1} + L_{j-1} - V_j - W_j - L_j - U_j = 0 \tag{1}$$

By adding up the mass balances across all stages, the overall (global) mass balance for the entire column is obtained.

$$\sum_{j=1}^{n} F_j - \sum_{j=1}^{n-1} \left(W_j + U_j \right) = 0 \tag{2}$$

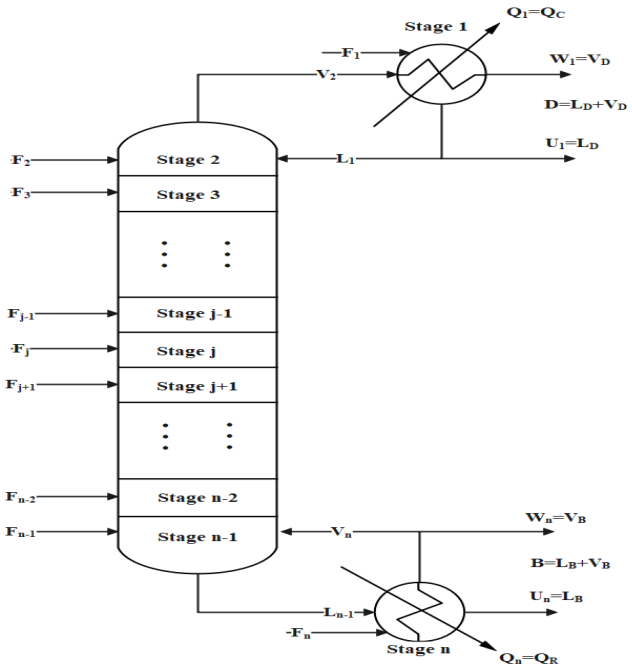


Figure 1. Schematic representation of a distillation column [16].

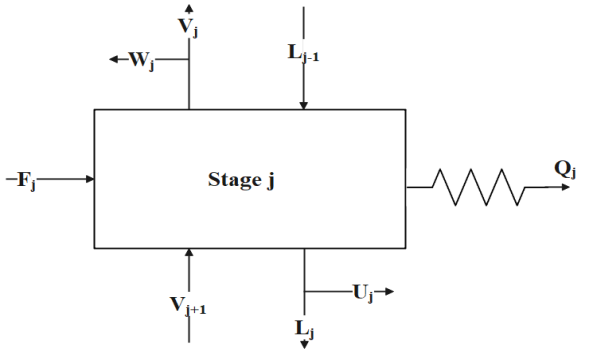


Figure 2. Schematic representation of input and output streams in a generic stage [16].

Alternatively, the overall mass balance can be expressed by explicitly separating the contributions of the distillate and bottoms streams, which correspond to the side streams located in the condenser and reboiler, respectively.

$$\sum_{j=1}^{n} F_j - B - D - \sum_{j=2}^{n-1}\left(W_j + U_j\right) = 0 \tag{3}$$

The component mass balance for species *i* on stage *j* can be expressed as follows:

$$z_{ij}F_j + y_{ij+1}V_{j+1} + x_{ij-1}L_{j-1} - y_{ij}(V_j + W_j) - x_{ij}(L_j + U_j) = 0 \tag{4}$$

Here, x_{ij} represents the mole fraction of component *i* in the liquid phase of stage *j*, y_{ij} denotes the mole fraction of component *i* in the vapor phase of stage *j*, and z_{ij} corresponds to the mole fraction of component *i* in the feed stream entering stage *j*.

The overall energy balance for stage *j*, neglecting variations in kinetic and potential energies, can be expressed as:

$$F_j H_j^F + V_{j+1}H_{j+1}^V + L_{j-1}H_{j-1}^L - (V_j + W_j)H_j^V - (L_j + U_j)H_j^L - Q_j = 0 \tag{5}$$

In this expression, H_j^F denotes the enthalpy of the feed stream entering stage *j*, H_j^V represents the enthalpy of the vapor stream leaving stage *j*, and H_j^L corresponds to the enthalpy of the liquid stream leaving stage *j*.

The overall energy balance for the column can be determined by summing the energy balances across all individual stages.

$$\sum_{j=1}^{n} F_j H_j^F - \sum_{j=1}^{n}(W_j H_j^V + U_j H_j^L + Q_j) = 0 \tag{6}$$

Alternatively, the global energy balance can be expressed in an equivalent form that explicitly accounts for the contributions of the distillate and bottoms streams.

$$\sum_{j=1}^{n} F_j H_j^F - L_B H_n^L - V_B H_n^V - L_D H_1^L - V_D H_1^V - Q_C - Q_R - \sum_{j=2}^{n-1}(W_j H_j^V + U_j H_j^L + Q_j) = 0 \tag{7}$$

The mass balance in a distillation column can be implemented using either a stage-equilibrium model or a rate-based (non-equilibrium) model. For this system, the parameters of the ternary mixture consisting of acetic acid, water, and the entrainers ethyl acetate and isobutyl acetate will be applied in the numerical simulation equations. Tables 1 and 2 present the values of the parameters required for this three-component system.

Table 1. Values of the parameters for the ternary water–acetic acid–ethyl acetate. mixture used in the NRTL model (ethyl acetate: 1, acetic acid: 2, water: 3).

i,j	A_{ij}	B_{ij}	B_{ji}
1,2	0.3	576	-322
1,3	0.3067	416	1024
2,3	0.3	-211	652

Table 2. Values of the parameters for the ternary water–acetic acid– isobutyl acetate. mixture used in the NRTL model (isobutyl acetate: 1, acetic acid: 2, water: 3).

i,j	A_{ij}	B_{ij}	B_{ji}
1,2	0.3	194	90
1,3	0.2505	489	1806
2,3	0.3	-211	652

In the non-random two-liquid (NRTL) activity coefficient model, which is commonly applied in the literature for non-ideal systems at pressures below 10 bar, an appropriate equation of state and the calculation of fugacity coefficients are required. To properly account for the dimerization of acetic acid in the vapor phase, the second virial coefficient equation of state with temperature-dependent parameters has been proposed. Moreover, for the estimation of fugacity coefficients, the Association method is employed, which is widely used in chemical engineering software such as Aspen Plus and MATLAB. In this MATLAB-based modeling, the virial equation of state is employed to describe the vapor phase behavior, particularly to account for acetic acid dimerization. For the liquid phase, the NRTL activity coefficient model is applied to represent the non-ideal behavior of the acetic acid-water-entrainer system. To determine the interaction parameters required for the system components (namely water-acetic acid, water-isobutyl acetate, and acetic acid-isobutyl acetate) data were obtained from the NIST Chemistry WebBook[17]. These interaction parameters are subsequently employed to calculate activity coefficients using the NRTL model, which is essential for accurately representing non-ideal behavior in the liquid phase during the numerical simulation of the heterogeneous azeotropic distillation process.

Fugacity represents the effective driving force of a substance in a chemical reaction and can be interpreted as its tendency to escape from the present phase. It quantifies the deviation of a real gas from ideal behavior and thus reflects its volatility and phase-transfer potential. In thermodynamic equilibrium, fugacity is defined as the pressure that an ideal gas would exert if it had the same chemical potential as the real gas at the actual conditions. The relationship between Gibbs free energy and pressure for a real gas introduces the concept of fugacity and its associated fugacity coefficient, which measures the degree of non-ideality. For mixtures, fugacity coefficients depend on temperature, pressure, and composition, and their ratios across phases determine phase-equilibrium constants. In this study, fugacities were calculated using the virial equation of state up to the second virial coefficient to accurately represent non-ideal behavior. The equilibrium equations were solved using the *fsolve* function in MATLAB, and a 70-tray distillation column model was employed to evaluate the phase separation performance.

The following assumptions were considered in this modeling study:

- Variations of concentrations and enthalpies with time are neglected (steady-state condition).
- The outlet streams from each stage are in vapor-liquid equilibrium.
- Energy variations in the reboiler and condenser with time are negligible.
- The column operates at a constant pressure.
- The NRTL thermodynamic model is used to calculate phase equilibrium and thermodynamic properties.

Mass and Energy Balance Equations:

1. Reboiler:

$$L_1 = B + V_B \tag{8}$$

$$L_1 x_1 = B x_B + V_B y_B \tag{9}$$

$$L_1 H_1^L + Q_R = B H_B^L + V_B H_B^V \quad (10)$$

2. First stage:

$$L_2 + V_B = L_1 + V_1 \quad (11)$$

$$L_2 x_2 + V_B y_B = L_1 x_1 + V_1 y_1 \quad (12)$$

$$L_2 H_2^L + V_B H_B^V = L_1 H_1^L + V_1 H_1^V \quad (13)$$

3. Intermediate stages (except feed and top stage):

$$L_{n+1} + V_{n-1} = L_n + V_n \quad (14)$$

$$L_{n+1} x_{n+1} + V_{n-1} y_{n-1} = L_n x_n + V_n y_n \quad (15)$$

$$L_{n+1} H_{n+1}^L + V_{n-1} H_{n-1}^V = L_n H_n^L + V_n H_n^V \quad (16)$$

4. Feed stage:

$$L_n^{F+1} + V_n^{F-1} + F = L_n^F + V_n^F \quad (17)$$

$$L_n^{F+1} x_n^{F+1} + V_n^{F-1} y_n^{F-1} + F x_F = L_n^F x_n^F + V_n^F y_n^F \quad (18)$$

$$L_n^{F+1} H_{L_n}^{F+1} + V_n^{F-1} H_{V_n}^{F-1} + F H_F = L_n^F H_{L_n}^F + V_n^F H_{V_n}^F \quad (19)$$

5. Top stage:

$$R + V_n^{T-1} = L_n^T + V_n^T \quad (20)$$

$$R x_D + V_n^{T-1} y_n^{T-1} = L_n^T x_n^T + V_n^T y_n^T \quad (21)$$

$$R H_D^L + V_n^{T-1} H_{V_n}^{T-1} = L_n^T H_{L_n}^T + V_n^T H_{V_n}^T \quad (22)$$

6. Condenser (reflux drum):

$$V_n^T = R + D \quad (23)$$

$$V_n^T y_n^T = (R + D) x_D + M x_M \quad (24)$$

$$V_n^T H_{V_n}^T = (R + D) H_{L_D} + Q_C \quad (25)$$

In these equations, the vapor and liquid flow rates are expressed in kmol/h, the enthalpies are given in kJ/kmol, and the heat duties (Q_R and Q_C) are reported in kJ/h. The phase equilibrium and thermodynamic properties, including vapor pressure, activity coefficients, and fugacity coefficients, were calculated using the NRTL model in combination with the Virial equation of state. The resulting complex system of mass and energy balance equations was then solved with the aid of MATLAB.

For the numerical simulation process using MATLAB, the governing mass and energy balance equations were first introduced at the inlet stage, along with the corresponding process stream flow rates. Mass and energy balances were then applied to each tray, with the outlet of one tray serving as the inlet for the next. For each component in the mixture (water, acetic acid, and the additive), an independent mass balance equation was formulated. Furthermore, the heat exchange between the vapor and liquid phases was incorporated through the thermodynamic relationships defined for each stage. By sequentially substituting these relationships into the equations of the subsequent trays, the acetic acid concentration in the vapor phase of the final stage was determined. Optimization of the process was achieved by varying inlet conditions, temperature profiles, and other operating parameters to maximize the acetic acid concentration in the bottom product stream. In cases where high purity could not be obtained in the bottom product, alternative strategies were employed, such as modifying the composition of the third component (ethyl acetate or isobutyl acetate), adjusting temperature and pressure conditions, or changing the compensating flow rate and additive composition. These adjustments disrupt the azeotropic mixture and enhance the transfer of acetic acid from the aqueous phase to the organic additive phase, thereby improving separation efficiency. The applied simulation algorithm followed four main steps: (1) introducing initial guess values, (2) calculating input parameters, (3) determining liquid compositions (x_{ij}) and component fractions using the defined equations, and (4) recalculating liquid compositions iteratively. Steps 2–4 were repeated until the changes in results became negligibly small.

2.2. Process Simulation Using Aspen Plus

The dehydration distillation column was simulated in Aspen Plus (version 12) using the RadFrac equilibrium model. The column was considered with 72 theoretical stages, including a kettle reboiler and a total condenser. The process was simulated under steady-state conditions to achieve azeotropic distillation and recover acetic acid with a purity of 96 wt% in the bottom stream. The overhead product consisted of a binary azeotropic mixture of water and isobutyl acetate, which, after condensation, was separated into aqueous and organic phases. The aqueous phase was directed to the subsequent purification section, while the organic phase was partially recycled to the column to enhance separation efficiency.

Multiple feed streams with different compositions and flow rates were introduced into the column at specified stages. These included vapor and liquid streams containing acetic acid, water, and organic entrainers. The thermodynamic properties were estimated using the NRTL activity coefficient model, which is widely applied for non-ideal liquid systems and azeotropic mixtures.

The simulation framework considered equilibrium between vapor and liquid phases at each stage, with mass and energy balances solved internally by Aspen Plus. Operating pressure was kept constant throughout the column, and temperature and composition profiles were monitored across the stages. The bottom product flow rate was adjusted to 53.043 kg/h, consistent with the plant design, while the top product flow rate was 100.950 kg/h.

Figure 3 illustrates the distillation column used for the separation of water and acetic acid, and the characteristics of the inlet and outlet streams to this column are presented in Tables 3 to 12.

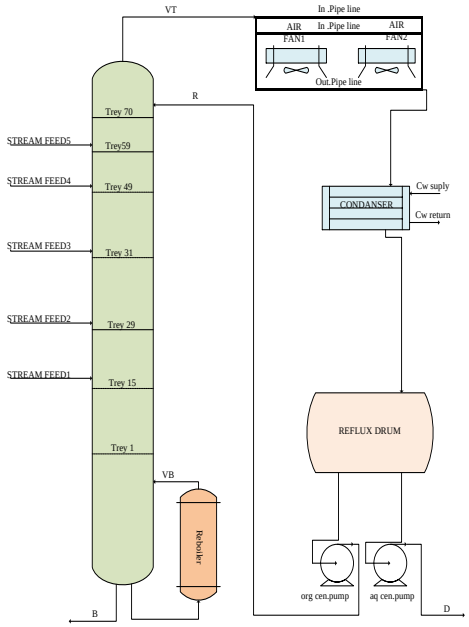


Figure 3. Water–acetic acid separation column.

Table 3. Feed 1 stream specifications of the water-acetic acid separation column.

Stream number	Stream feed 1	
State	Vapor	
Temperature (°C)	124	
Pressure (bar g	0.6	
Compositions	Kg/h	%wt
Acetic acid	16777.3	83.6
Isobutyl acetate	0	0
Water	3110.7	16.4
Flowrate	20052.4	-
Molecular weight (kg/kmol)	44.1	
Density (kg/m^3)	2.8	
Enthalpy (kw)	5459	
Specific heat capacity (kJ/kg.K)	1.40	
Viscosity (m pa.s)	0.0115	

Table 4. Feed 2 stream specifications of the water-acetic acid separation column.

Stream number	Stream feed 2	
State	Vapor	
Temperature (°C)	156	
Pressure (bar g	3.00	
Compositions	Kg/h	%wt
Acetic acid	15689.1	81.8
Isobutyl acetate	0	0
Water	3245	18.2
Flowrate	19189.1	-
Molecular weight (kg/kmol)	43.1	
Density (kg/m^3)	6	
Enthalpy (kw)	5817	
Specific heat capacity (kJ/kg.K)	1.45	
Viscosity (m pa.s)	0.00130	

Table 5. Feed 3 stream specifications of the water-acetic acid separation column.

Stream number	Stream feed 3	
State	Vapor	
Temperature (°C)	129	
Pressure (bar g	11.97	
Compositions	Kg/h	%wt
Acetic acid	7165.2	77
Isobutyl acetate	0	0
Water	1975.4	23
Flowrate	9307	-
Molecular weight (kg/kmol)	67.05	
Density (kg/m^3)	923.7	
Enthalpy (kw)	873	
Specific heat capacity (kJ/kg.K)	2.40	
Viscosity (m pa.s)	0.2789	

Table 6. Feed 4 stream specifications of the water-acetic acid separation column.

Stream number	Stream feed 4	
State	Liquid	
Temperature (°C)	57	
Pressure (bar g	0.17	
Compositions	Kg/h	%wt
Acetic acid	11314.7	48.13
Isobutyl acetate	33.2	0.17
Water	12157.2	51.7
Flowrate	24613.9	-
Molecular weight (kg/kmol)	27.21	
Density (kg/m^3)	897	
Enthalpy (kw)	1189	
Specific heat capacity (kJ/kg.K)	3.17	
Viscosity (m pa.s)	0.5355	

Table 7. Feed 5 stream specifications of the water-acetic acid separation column.

Stream number	Stream feed 5	
State	Vapor	
Temperature (°C)	119	
Pressure (bar g	0.10	
Compositions	Kg/h	%wt
Acetic acid	47.6	9.1
Isobutyl acetate	5.2	1
Water	412.4	78.7
Flowrate	524.3	-
Molecular weight (kg/kmol)	100.9	
Density (kg/m^3)	3.7	
Enthalpy (kw)	89	
Specific heat capacity (kJ/kg.K)	1.60	
Viscosity (m pa.s)	0.0091	

Table 8. R stream specifications of the water–acetic acid separation column.

Stream number	Stream R	
State	Liquid	
Temperature (°C)	49	
Pressure (bar g	0.07	
Compositions	Kg/h	%wt
Acetic acid	88	0.1
Isobutyl acetate	1652.4	2.1
Water	61641.5	76.6
Flowrate	80424.9	–
Molecular weight (kg/kmol)	101.6	
Density (kg/m^3)	850.1	
Enthalpy (kw)	2239	
Specific heat capacity (kJ/kg.K)	2.04	
Viscosity (m pa.s)	0.4563	

Table 9. Stream V_B specifications of the water–acetic acid separation column.

Stream number	Stream V_B	
State	Vapor	
Temperature (°C)	127	
Pressure (bar g	0.6	
Compositions	Kg/h	%wt
Water	24537.7	100
Flowrate	24537.7	-

Table 10. Stream D specifications of the water–acetic acid separation column.

Stream number	Stream D	
State	Liquid	
Temperature (°C)	45	
Pressure (bar g	5.0	
Compositions	Kg/h	%wt
Acetic acid	10.9	0.1
Isobutyl acetate	154.0	0.8
Water	18370.9	96.1
Flowrate	19123.8	-
Molecular weight (kg/kmol)	18.62	
Density (kg/m^3)	977.3	
Enthalpy (kw)	964	
Specific heat capacity (kJ/kg.K)	4.09	
Viscosity (m pa.s)	0.6056	

Table 11. Stream B specifications of the water–acetic acid separation column.

Stream number	Stream B	
State	Liquid	
Temperature (°C)	127	
Pressure (bar g	0.6	
Compositions	Kg/h	%wt
Acetic acid	50934.2	96.0
Isobutyl acetate	0	0
Water	2108.8	4.0
Flowrate	53043	-
Molecular weight (kg/kmol)	52.44	
Density (kg/m^3)	928	
Enthalpy (kw)	4358	
Specific heat capacity (kJ/kg.K)	2.6	
Viscosity (m pa.s)	0.3390	

Table 12. Stream V_T specifications of the water–acetic acid separation column.

Stream number	Stream V_T	
State	Vapor	
Temperature (°C)	85	
Pressure (bar g	0.07	
Compositions	Kg/h	%wt
Acetic acid	98.8	0.1
Isobutyl acetate	61672.2	61.3
Water	20032.5	19.9
Flowrate	100530.7	-
Molecular weight (kg/kmol)	53.6	
Density (kg/m^3)	2	
Enthalpy (kw)	25638	
Specific heat capacity (kJ/kg.K)	1.67	
Viscosity (m pa.s)	0.0097	

A schematic representation of the simulated distillation column is shown in Figure 4, and the detailed column specifications are summarized in Table 13.

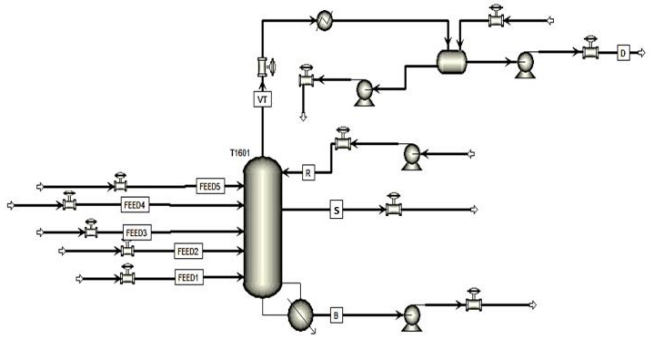


Figure 4. A schematic representation of the simulated distillation column in Aspen Plus (V12).

Table 13. Distillation column specifications

Specification	Value
Number of stages	70
Bottom temperature (°C)	127
Top temperature (°C)	89
Distillate mass flow rate (kg/h)	100.950
Bottoms mass flow rate (kg/h)	53.043
Internal Type	Trayed
Tray Type	Sieve
Number of Passes	2
Tray Spacing (m)	0.6096
Diameter (m)	3.214

3. Result and Discussion

3.1. Effect of Additives and Optimization Using MATLAB

In this section, the results obtained from the modeled data of the distillation column in MATLAB are analyzed and compared with the design data of the industrial unit. Table 14 presents the temperature profiles of trays 1, 5, 50, and 70 for both the design case and the simulated cases using two different entrainers: isobutyl acetate (IBA)—which is currently used in the real process—and ethyl acetate (EA), proposed in this study as a potential alternative. As shown in the table, the simulated temperature profile for the IBA case closely follows the design data, confirming the accuracy of the developed model. The simulated bottom temperature of 121.9°C is approximately 5°C lower than the design value (127°C), corresponding to a relative deviation of about 4%. This moderate reduction implies a slightly lower reboiler duty, which may translate into energy savings without compromising product purity. At the top of the column, the simulated temperature (92°C) is about 7°C higher than the design value (85°C), resulting in an 8% relative error. Such deviations are likely due to simplifying assumptions in vapor–liquid equilibrium and tray efficiency correlations within the MATLAB model. For the EA case, larger discrepancies from the design data are observed. The simulated bottom temperature (116.5°C) shows a difference of 10.5°C (8.2% relative error), while the top temperature (86°C) deviates by only 1% from the design. These results indicate that using ethyl acetate as an entrainer alters the internal temperature distribution, reducing the temperature gradient across the column and potentially affecting the driving force for mass transfer.

A comparative analysis of the two entrainers suggests that isobutyl acetate provides better thermal consistency with the design data, ensuring more stable operation and effective separation of acetic acid. In contrast, ethyl acetate, though lighter and more volatile, causes higher deviations, particularly in the bottom section, which could impact separation efficiency. Overall, the comparison validates the robustness of the developed model and demonstrates that the column simulated with isobutyl acetate accurately replicates real operational behavior. However, the ethyl acetate case, despite showing larger temperature deviations, may still offer operational benefits such as reduced reboiler duty or lower solvent cost, which require further techno-economic evaluation.

Table 14. Comparison of tray temperature distribution between design and simulation.

Tray number	Design temperature (°C)	Simulated temperature (°C) (IBA)	Simulated temperature (°C) (EA)
1	127	121.9	116.5
5	123	120	109.3
50	96	107.9	104.7
70	85	92	86

Figure 5a and 5b illustrate the simulated profiles of acetic acid mole fraction in the liquid and vapor phases along the 70 equilibrium stages of the column when using isobutyl acetate (IBA) and ethyl acetate (EA) as entrainers. In the liquid phase (Figure 5a), the acetic acid mole fraction decreases from 0.78 (IBA) and 0.80 (EA) at the bottom (stage 1) to 0.11 (IBA) and 0.18 (EA) at the top (stage 70), reflecting the progressive removal of acetic acid through vaporization and its subsequent condensation with the entrainer. The similarity of the two profiles indicates that both entrainers effectively facilitate the azeotrope-breaking process; however, the slightly lower top-stage concentration obtained with IBA suggests that it provides stronger interaction with acetic acid, thereby enhancing the retention of acid in the liquid phase and improving the overall separation efficiency. The vapor-phase profiles (Figure 5b) exhibit complementary behavior, with the acetic acid mole fraction decreasing from 0.55 (IBA) and 0.63 (EA) at stage 1 to 0.08 (IBA) and 0.06 (EA) at stage 70. The somewhat higher vapor-phase acid concentration in the presence of EA can be attributed to its higher volatility and weaker association with acetic acid, which promotes partial entrainment of acid into the vapor stream. In contrast, IBA, being less volatile and more hydrophobic, stabilizes the acid in the liquid phase and reduces its transfer to the top product. Several inflection points are observed along both the liquid and vapor concentration profiles. These correspond to the feed tray locations, where the introduction of streams with different temperatures and compositions temporarily disturbs the local vapor–liquid equilibrium. Minor oscillations may also arise from the non-ideal distribution of the entrainer along the column, local variations in tray efficiency, and model simplifications in the thermodynamic framework (NRTL parameters). Despite these small fluctuations, the overall consistency and smooth convergence of both curves confirm that the model provides a reliable representation of the column's steady-state behavior. The comparative analysis between IBA and EA indicates that IBA slightly outperforms EA in achieving higher acetic acid purity at the column bottom and lower acid content at the top. This improvement can be rationalized by the stronger non-ideal interactions between IBA and acetic acid, as well as the lower relative volatility of IBA, which enhance the driving force for acetic acid retention in the reboiler region. These results align well with the literature on heterogeneous azeotropic distillation, where heavier esters generally provide better phase separation and higher product purities under similar operating conditions [18, 19].

Figure 6 presents the time-dependent evolution of acetic acid composition in both the bottom and top product streams of the column for two entrainers, isobutyl acetate (IBA) and ethyl acetate (EA). In Figure 6(a), the liquid-phase acetic acid concentration in the bottom product gradually increases during the simulation and reaches a steady-state value of 0.87 for IBA and 0.85 for EA after approximately 15 hours of operation. This monotonic increase indicates the gradual removal of water and entrainer from the bottom section, which enhances the relative volatility difference between acetic acid and the light components, leading to an increase in product purity. The model successfully captures the transient-to-steady-state transition of the system, confirming its reliability in describing the column's dynamic behavior. The slightly higher final purity obtained with IBA suggests a stronger entraining effect and higher azeotrope-breaking efficiency, primarily due to IBA's lower miscibility with water and its ability to create a more distinct vapor–liquid equilibrium boundary. Consequently, mass transfer between the phases is enhanced, resulting in sharper separation and improved bottom product quality. Although EA achieves a slightly lower steady-state concentration (0.85), the deviation (around 2%) remains small, indicating that EA can still act as a viable and energy-efficient alternative to IBA under optimized operating conditions. In Figure 6(b), the temporal evolution of acetic acid concentration in the top vapor product is illustrated. The acetic acid mole fraction increases from 0.01 to 0.18 when IBA is used and from 0.01 to 0.12 when EA is used as the entrainer. The gradual increase over time reflects the progressive enrichment of the vapor phase with acetic acid as equilibrium is established throughout the column. The higher top-product acetic acid concentration in the IBA case again confirms its stronger affinity for acetic acid in the vapor phase, enhancing its ability to break the azeotrope and facilitate mass transfer. In contrast, the lower vapor-phase concentration in the EA system suggests that acetic acid is more effectively retained in the liquid phase, which is consistent with its slightly higher polarity and better solubility in aqueous mixtures. Overall, the results in both subfigures demonstrate consistent dynamic trends and confirm that while IBA provides a slightly better overall separation efficiency, EA remains an effective and practical substitute that maintains stable operation and acceptable product quality. These observations validate the thermodynamic accuracy and predictive capability of the developed MATLAB model for both steady-state and transient analyses of the distillation process.

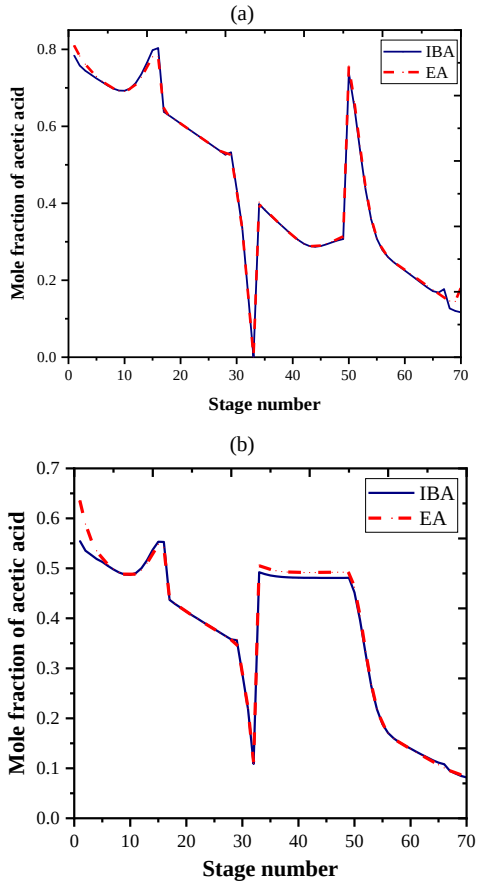


Figure 5. (a) Liquid-phase acetic acid mole fraction along the column stages for isobutyl acetate and ethyl acetate entrainers, (b) Vapor-phase acetic acid mole fraction along the column stages for the same systems.

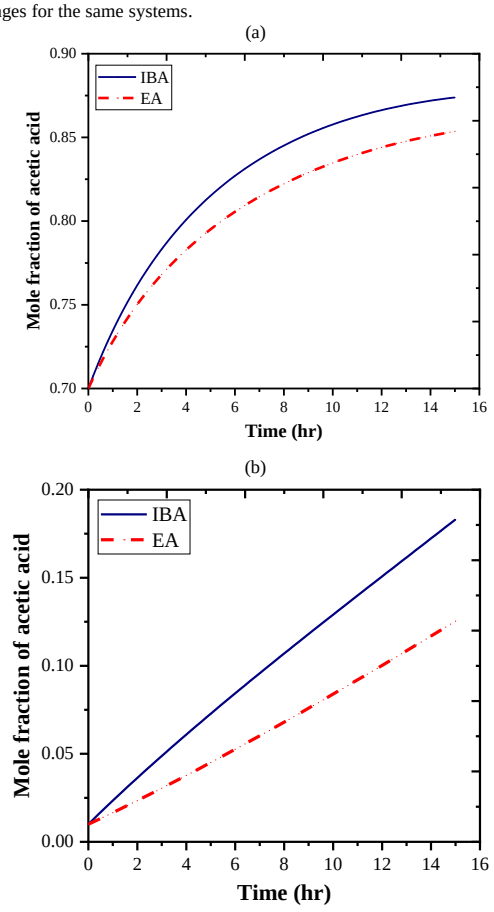


Figure 6. (a) Temporal variation of acetic acid mole fraction in the bottom liquid product, (b) Temporal variation of acetic acid mole fraction in the top vapor product for isobutyl acetate and ethyl acetate entrainers.

Figure 7 illustrates the variation of water mole fraction in both liquid and vapor phases along the column stages for the two entrainers. As shown in Figure 7(a), the liquid-phase water content gradually increases from approximately 0.13 at the column bottom (stage 1) to nearly 1.0 at the top (stage 70) for both ethyl acetate and isobutyl acetate. This steady increase indicates the efficient stripping of water toward the top of the column, consistent with the desired dehydration trend. The small difference between the two entrainers suggests that both systems exhibit similar phase equilibrium characteristics in the liquid phase, which is attributed to their comparable volatility and interaction strength with water. In Figure 7(b), the vapor-phase water mole fraction shows a similar ascending profile, starting from 0.19 (ethyl acetate) and 0.17 (isobutyl acetate) at the bottom and reaching 0.71 and 1.2, respectively, at the top of the column. The slightly higher vapor-phase water concentration in the presence of isobutyl acetate indicates its stronger capacity to promote water transfer into the vapor phase due to its lower volatility and higher affinity for water at elevated stages. The observed breakpoints along both curves correspond to the feed and entrainer injection stages, where the local composition and vapor–liquid equilibrium conditions change abruptly, leading to sharp composition gradients. These fluctuations are typical in reactive or extractive distillation processes and confirm that the model successfully captures the effect of feed distribution and entrainer addition on internal mass transfer.

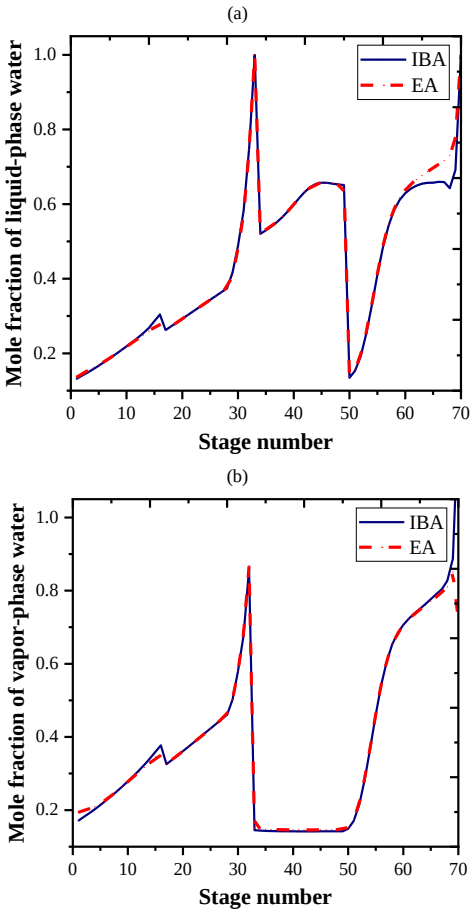


Figure 7. (a) Liquid-phase water mole fraction along the column stages for isobutyl acetate and ethyl acetate entrainers, (b) Vapor-phase water mole fraction along the column stages for the same systems.

Figure 8(a) presents the temporal variation of the water mole fraction in the bottom product. The water content decreases continuously over time, indicating the progressive removal of water from the reboiler region and the system's approach toward steady-state operation. For ethyl acetate, the mole fraction decreases from 0.30 to approximately 0.17, whereas for isobutyl acetate it declines from 0.26 to about 0.15. The lower final value observed with isobutyl acetate suggests slightly better water removal efficiency, which can be attributed to its higher boiling point and stronger interaction with acetic acid, resulting in improved phase separation and enhanced dehydration at the bottom section. Figure 8(b) compares the water mole fraction in the distillate stream for both entrainers. The water content in the vapor product increases from 0.80 to 0.91 for ethyl acetate and from 0.80 to 0.97 for isobutyl acetate, reflecting the more effective transfer of water into the top vapor stream when isobutyl acetate is used. This trend corroborates the vapor-phase results shown in Figure 7(b) and further confirms that isobutyl acetate facilitates higher water stripping efficiency. Overall, the combined trends in Figures 7 and 8 demonstrate that both entrainers effectively enhance dehydration performance, with isobutyl acetate showing a marginally superior behavior due to its thermodynamic properties and mass-transfer advantages.

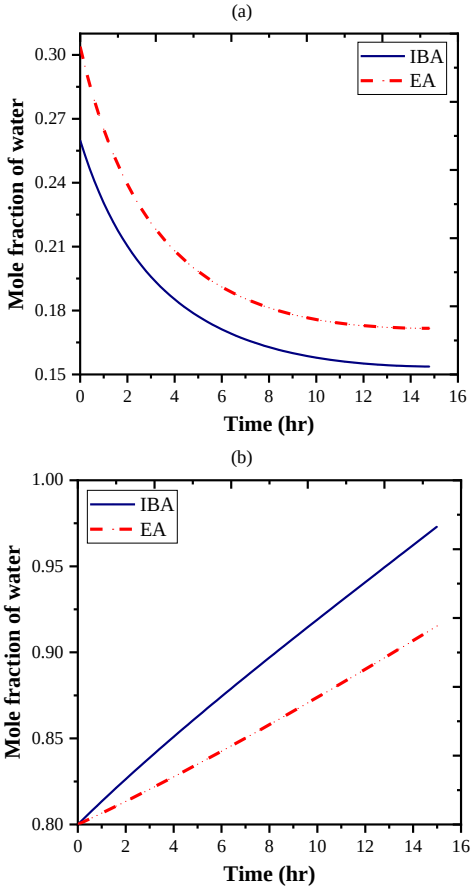


Figure 8. (a) Variation of liquid-phase water mole fraction in the bottom product with time for both entrainers, (b) Water mole fraction in the distillate for ethyl acetate and isobutyl acetate entrainers.

Figure 9 presents the variation of the entrainer mole fraction (isobutyl acetate and ethyl acetate) along the distillation column stages. As observed, both entrainers show a gradual decrease in concentration from the bottom (stage 1) toward the top (stage 70) of the column, eventually approaching zero at the condenser outlet. For isobutyl acetate, the liquid-phase mole fraction decreases from 0.08 at stage 1 to nearly 0 at stage 70, while for ethyl acetate, it decreases from 0.05 to 0 over the same range. This behavior confirms the effective stripping and recovery of the entrainer during the distillation process, as most of it vaporizes and exits with the overhead stream. The slightly higher concentration of isobutyl acetate at the lower trays indicates its lower volatility and stronger affinity toward the liquid phase compared to ethyl acetate, which exhibits a slightly faster decline along the column due to its higher vapor pressure and lower molecular weight. The overall similarity of the two curves suggests that both entrainers follow a comparable distribution profile along the column, indicating that substituting ethyl acetate for isobutyl acetate does not significantly alter the mass-transfer and phase-equilibrium characteristics of the system. The minor differences observed are primarily due to variations in the relative volatility and interaction parameters between each entrainer and water/acetic acid mixtures. Therefore, while isobutyl acetate ensures slightly better control of the separation interface, ethyl acetate remains a feasible alternative under comparable operating conditions, especially in energy-sensitive operations.

The effect of reflux ratio on the reboiler duty and the top product water composition was evaluated to identify the optimal operational conditions of the distillation column. As illustrated in Figure 10(a), the top product water mole fraction increases with the reflux ratio up to approximately 1.5. Beyond this point, further increases in reflux ratio have a negligible effect on the product purity, with the water mole fraction stabilizing around 0.97. This indicates that the column has effectively reached its separation capacity, and increasing reflux beyond this point does not significantly improve water removal. Based on this observation, the optimum reflux ratio was determined to be 1.5. Subsequently, the corresponding reboiler duty was analyzed as a function of reflux ratio (Figure 10(b)). It can be seen that at reflux ratios lower than 1.5, the reboiler duty rises moderately with increasing reflux ratio, reflecting the additional energy required to vaporize the larger liquid flow circulated in the column. Once the reflux ratio exceeds the optimal value of 1.5, the reboiler

duty increases sharply, imposing significant energy consumption without substantial improvement in separation performance. These trends indicate that operating at a reflux ratio of 1.5 provides an optimal balance between energy consumption and separation efficiency, ensuring high water removal in the top product while minimizing unnecessary reboiler load. Furthermore, the comparison between IBA and EA shows that while the curves are very close, IBA offers slightly better separation efficiency with marginally lower reboiler duty, confirming its superior entraining effect. Nonetheless, EA can still be considered a feasible alternative under optimized reflux conditions.

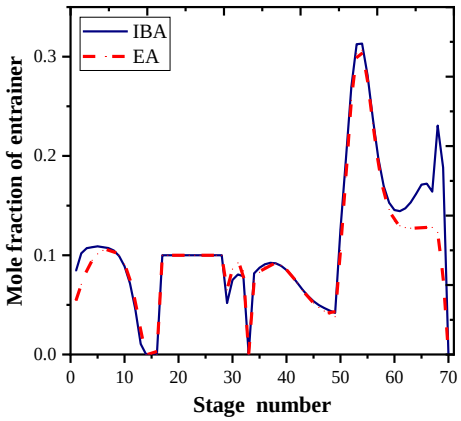


Figure 9. Variation of entrainer (isobutyl acetate and ethyl acetate) mole fraction along the column stages.

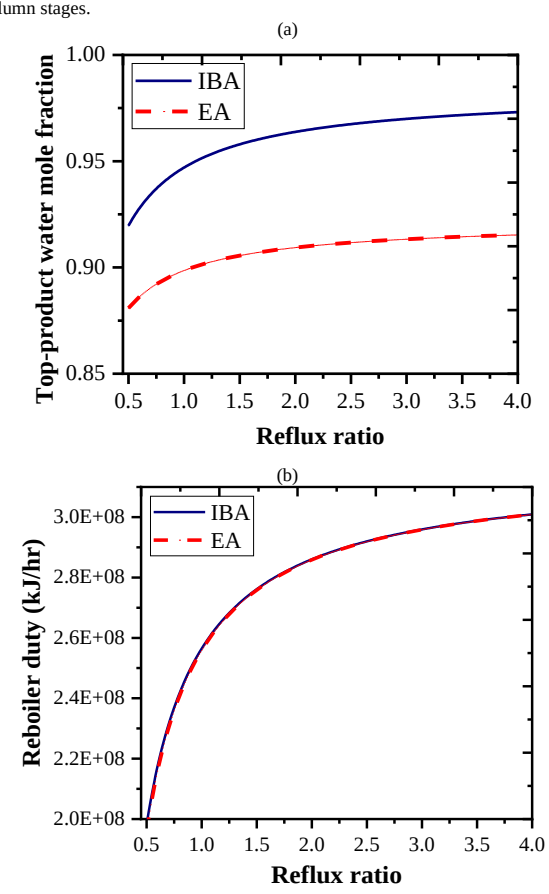


Figure 10. (a) Top product water mole fraction vs. reflux ratio, (b) Reboiler duty vs. reflux ratio, for isobutyl acetate (IBA) and ethyl acetate (EA).

3.2. Process Simulation of the Acetic Acid-Water Distillation Column Using Aspen Plus

In this section, the simulation of the acetic acid-water distillation column was performed using Aspen Plus (version 12). The specifications of the feed streams entering the column are presented in Table 15 and schematically in Figure 4. The column was modeled using the RadFrac absorption module with a Kettle-type reboiler, and a bottom product mass flow rate of 53,043 kg/h was considered. The simulation was carried out under equilibrium conditions with 72 theoretical stages, while a total column pressure drop of 1 bar was included. The feed entry points and their respective stages are detailed in Table 16, illustrating how each feed stream interacts with the internal stages of the column. The resulting outlet streams from the column, including both top and bottom products, are summarized in Table 17.

The simulation results indicate that the RadFrac model can effectively capture the internal stage compositions and temperature profiles, providing detailed insights into the separation efficiency along the column height. The choice of 72 stages ensures adequate resolution of concentration gradients, particularly for the acetic acid-rich bottom product and the water-rich top product. The incorporation of a small pressure drop (1 bar) reflects realistic column operation, slightly influencing the vapor-liquid equilibrium and thus the predicted product purities. Overall, the simulated results demonstrate the feasibility of achieving the desired acetic acid purity in the bottom product while maintaining operational stability, providing a reliable basis for further process optimization and comparison with experimental or design data.

Table 15. Specifications of feed streams entering the acetic acid–water distillation column.

Stream number	Temperature (°C)	Pressure (bar)	Acetic Acid (mole frac.)	Isobutyl Acetate (mole frac.)	Water (mole frac.)	Mass flow rate (kg/hr)
Feed 1	124	1.7	0.62	0	0.38	19887
Feed 2	156	1.59	0.6	0	0.41	18934
Feed 3	129	1.56	0.87	0.124	0	136.3
Feed 4	57	1.3	0.22	0.00033	0.78	23504
Feed 5	117.7	1.16	0.17	0.766	0.062	465
R	45.4	1.01	0.00056	0.85	0.147	63313

Table 16. Feed entry locations in the acetic acid–water distillation column.

Stream number	Stage	Convention
Feed 1	56	Above stage
Feed 2	42	Above stage
Feed 3	40	Above stage
Feed 4	22	Above stage
Feed 5	12	Above stage
R	1	Above stage

Table 17. Outlet streams from the acetic acid–water distillation column.

Stream number	Temperature (°C)	Pressure (bar)	Acetic Acid (mole frac.)	Isobutyl Acetate (mole frac.)	Water (mole frac.)	Mass flow rate (kg/hr)
VT	93	1.01	0.0150997	0.368731	0.616169	81663
S	110.69	1.3	0.210203	0.000959533	0.788833	538
B	137.4	2.01	0.8135	0.00235247	0.184149	53043

4. Conclusions

The simulation of the acetic acid–water distillation column was conducted to evaluate the performance of the separation process and to compare the behavior of two different entrainers, isobutyl acetate (IBA) and ethyl acetate (EA). The results showed that the bottom stream acetic acid purity reached approximately 0.82 mole fraction when IBA was used, while a slightly lower value of 0.78 was obtained with EA. The top vapor stream contained around 0.95 mole fraction of water, confirming efficient phase separation and good agreement with expected process performance. Minor deviations can be attributed to trace volatile components such as methyl acetate and paraxylene that slightly affect vapor–liquid equilibrium. Temperature and composition profiles along the column indicated that IBA provides a more stable and sharper separation boundary, leading to higher acetic acid purity and better azeotrope-breaking efficiency compared with EA. However, EA still demonstrated acceptable separation capability, confirming its potential as a feasible alternative entrainer in cases where process simplification or solvent availability is prioritized. The effect of reflux ratio on both reboiler duty and water purity in the distillate was also investigated. As the reflux ratio increased from 0.5 to 1.5, the reboiler duty rose sharply due to enhanced internal liquid circulation. Beyond a reflux ratio of 1.5, the rate of increase in reboiler duty diminished, while the water mole fraction in the distillate remained nearly constant (~0.97). This behavior indicates that further increasing the reflux ratio above 1.5 does not significantly improve product purity but leads to unnecessary energy consumption. Therefore, a reflux ratio of 1.5 was determined as the optimum operating condition, providing the best trade-off between energy efficiency and product quality. Also, he simulation of the acetic acid–water distillation column was performed to evaluate the performance of the separation process and to compare the behavior of two different entrainers, isobutyl acetate (IBA) and ethyl acetate (EA).

In summary, the simulation results demonstrate that isobutyl acetate achieves better separation performance and energy utilization for the acetic acid–water system. Nevertheless, ethyl acetate can also serve as a practical substitute without requiring equipment modification, provided that operational parameters-particularly the reflux ratio-are properly optimized. These findings emphasize the importance of entrainer selection and reflux optimization in achieving energy-efficient and cost-effective distillation processes.

Credit Authorship Contribution Statement

Mahyar Daneshyar and Sara Abbasi: Investigation and perform calculations, Mohammad Reza Khosravi-Nikou: Supervision, Project administration, and Manuscript writing and editing results.

Conflicts of Interest

The authors declare that they do not have any personal or financial conflicts of interest.

References

[1] M. L. Luyben, B. D. Tyréus, *Computers & Chemical Engineering*, 1998, **22(7-8),** 867-877.

[2] J. Golob, V. Grilc, B. Zadnik, *Industrial & Engineering Chemistry Process Design and Development*, 1981, **20(3),** 433-435.

[3] R. W. Helsel, *Waste Recovery: Removing Carboxylic Acids From Aqueous Wastes*, 1977.

[4] Y. Kuo, H. P. Gregor, *Separation Science and Technology*, 1983, **18(5),** 421-440.

[5] D. F. Othmer, *Chemical Engineering Progress*, 1963, **59(6),** 67-78.

[6] J. Mills, *ACM Computing Surveys*, 1996, **28(4es),** 31. doi: 10.1145/242224.242263.

[7] S. K. Wasylkiewicz, L. C. Kobylka, F. J. L. Castillo, *Chemical Engineering Journal*, 2000, **79(3),** 219-227.

[8] T. Kurooka, Y. Yamashita, H. Nishitani, Y. Hashimoto, M. Yoshida, M. Numata, *Computers & Chemical Engineering*, 2000, **24,** 887-892. doi: 10.1016/S0098-1354(00)00346-X.

[9] S. J. Wang, K. Huang, *Chemical Engineering and Processing: Process Intensification*, 2012, **60(21),** 65-76. doi: 10.1016/j.cep.2012.05.006.

[10] J. J. Siirola, *AIChE Symposium Series*, 1995, **91(304),** 222-234.

[11] J. G. Hayden, J. P. O'Connell, *Industrial & Engineering Chemistry Process Design and Development*, 1975, **14(3),** 209-216.

[12] H. Wang, ournal of the American Oil Chemists' Society, 1973, **116(2),** 229-250, Accessed: Jan. 29, 2025. [Online]. Available: https://pubs.acs.org/sharingguidelines%0A https://pubs.acs.org/doi/book/10.1021/ba-1973-0116

[13] J. Gmehling, Vapor-Liquid Equilibrium Data Collection, Part 1-8, *Dechema Chemistry Data Series*, 1977.

[14] T. Magnussen, J. M. Sørensen, P. Rasmussen, A. Fredenslund, *Fluid Phase Equilibria*, 1980, **4(1),** 151-163. doi: https://doi.org/10.1016/0378-3812(80)80012-4.

[15] H. Renon, J. M. Prausnitz, *American Institute of Chemical Engineers (AIChE)*, 1968, **14(1),** 135-144.

[16] V. Steffen, E. A. da Silva, *Distill. Appl. Model*., 2017.

[17] National Institute of Standards and Technology | NIST. Accessed: Decamber 22, 2023. [Online]. Available: https://www.nist.gov/

[18] I. Rodriguez, V. Gerbaud, X. Joulia, *Industrial & Engineering Chemistry Research*, 2009, **51.** doi: 10.1021/ie801060n.

[19] S. Skouras, V. Kiva, S. Skogestad, *Chemical Engineering Science*, 2005, **60(11)** 2895-2909.